Chemical Engineering Journal 162 (2010) 28–36

Contents lists available at ScienceDirect

Chemical Engineering Journal

journal homepage: www.elsevier.com/locate/cej

Sol–gel derived poly(vinyl alcohol)-3-(2-aminoethylamino) propyl trimethoxysilane: Cross-linked organic–inorganic hybrid beads for the removal of Pb(II) from aqueous solution

S. Prakash, Mahendra Kumar, Bijay P. Tripathi, Vinod K. Shahi*

Electro-Membrane Processes Division, Central Salt & Marine Chemicals Research Institute, Council of Scientific & Industrial Research (CSIR), G.B. Marg, Bhavnagar 364002, Gujarat, India

ARTICLE INFO

Article history:
Received 10 February 2010
Received in revised form 11 April 2010
Accepted 27 April 2010

Keywords:
Adsorption
Pb(II) ion
Langmuir and Freundlich isotherms
PVA-AEAPTMEOS beads
Cross-linking

ABSTRACT

This manuscript reports sol–gel derived cross-linked poly(vinyl alcohol) (PVA)-3-(2-aminoethylamino) propyl trimethoxysilane (AEAPTMEOS) beads with low degree of swelling as a new adsorbent for the removal of Pb(II) from aqueous solution. Beads were prepared by condensation polymerization followed via acid-catalyzed sol–gel process in presence of non-ionic surfactant. Cross-linking was achieved by glutaraldehyde. Presence of –NH/–NH_2 groups in beads provide active sites for Pb(II) adsorption, and were responsible for high adsorption capacity. SEM/TEM studies confirmed the spherical and rough surface morphology, which was changed after Pb(II) adsorption. For the removal of Pb(II) in aqueous solution, effect of equilibrium time, temperature, pH, adsorbent dose and adsorbate concentration were investigated in batch process. Pseudo-first- and pseudo-second-order kinetics were also evaluated. The equilibrium adsorption followed Langmuir and Freundlich isotherms. Thermodynamic parameters such as ΔG°, ΔH° and ΔS° revealed endothermic and spontaneous adsorption. Monolayer adsorption capacity (Q_0) value for the developed PVA-AEAPTMEOS beads was 67.56 mg g^{-1} at pH: 5.0, much higher as compared to other adsorbents reported in literature. Desorption studies also suggested that cross-linked PVA-AEAPTMEOS beads can be effectively utilized for the removal of Pb(II) from wastewater.

1. Introduction

The presence of toxic heavy metal ions in industrial effluents or drinking water is serious environmental problem [1]. The most common heavy metals (Cr, Ni, Mn, Hg, Cd, Pb, Cu and Zn) found in industrial wastewater are not biodegradable. Thus, there is necessary for their removal either by physical or chemical methods from contaminated water [2–4]. Pb(II) pollution aroused due to use of Pb in service pipes, particularly with soft water, battery industry, auto-exhaust, paints, etc. The maximum allowable concentration of Pb(II) in drinking water is 0.1 mg dm^{-3}. Pb(II) contamination causes poisoning, nervous and renal breakdown, headache, brain damage, convulsions behavioral disorders and constipation [5–7]. Thus, removal of Pb(II) is important for the protection of environmental quality and public health [8]. The traditional methods, such as ion-exchange, solvent extraction, chemical precipitation, electrochemical reduction, and reverse osmosis were commonly used for the removal of heavy metal ions from wastewater [9–12]. Also, neutralization and precipitation of metal hydroxide are widely used techniques. Disposal of metal containing sludge is one of the main drawbacks of this technique. Thus, economically feasible and eco-friendly methods are necessary for wastewater treatments.

A number of adsorbents were used for the removal of heavy metal ions from wastewater [13–16]. During last three decades, activated carbon was frequently used as adsorbent, but it was not cost effective. Thus, developments of low cost adsorbent for the removal of heavy metal ions from wastewater, was highly attractive in recent years [17,18]. Chitosan/PVA blended beads were extensively studied for biomedical applications and lead adsorption, due to their good mechanical and chemical properties [8,19,20]. The cross-linked or blended chitosan beads were highly water swollen (water content > 19%) and showed poor mechanical strength for their practical applications [19]. The organic–inorganic hybrid materials were also attractive because of their attractive mechanically properties, thermally stable inorganic backbone, the specific chemical reactivity and flexibility of the organic functional groups [21–23]. Properties of hybrid materials were depended on their structural, dynamic properties and chemical composition. Number of organic–inorganic hybrid adsorbents such as MCM-41, polymer-supported nanosized hydrous manganese dioxide (HMO), silica nanospheres, MCM-41 modified by alumina and pyrimidine-

* Corresponding author. Tel.: +91 278 2569445; fax: +91 278 2567562/2566970.
E-mail address: vkshahi@csmcri.org (V.K. Shahi).

1385-8947/$ – see front matter © 2010 Elsevier B.V. All rights reserved.
doi:10.1016/j.cej.2010.04.048

derivated mesoporous materials, etc., were reported for heavy metal ions removal from wastewater [24–30]. But suitable tailoring of organic–inorganic hybrid materials by introducing –NH/–NH_2 groups (containing lone pair of electron responsible for metal ion adsorption) as active sites may provide an efficient adsorbent with high affinity for the removal of heavy metal ions (such as Pb(II)).

Herein, we are reporting sol–gel derived cross-linked PVA-AEAPTMEOS organic–inorganic hybrid beads with low water content for the removal of Pb(II) from wastewater. Applicability of developed beads for the removal of Pb(II) from aqueous solution was tested in laboratory scale experiments. Presence of –NH/–NH_2 groups provides active sites for Pb(II) removal from aqueous solution. Pb(II) adsorption capacity was explored under different experimental conditions and compared with the reported values in literature.

2. Experimental

2.1. Materials

AEAPTMEOS was obtained from Sigma–Aldrich Chemicals. Poly(vinyl alcohol) (PVA, Mw: 125,000, degree of polymerization: 1700, degree of hydrolysis: 88%), Span-80, $Pb(NO_3)_2$, erichrome black-T, ethylenediaminetetraacetic acid disodium salt (Na_2EDTA) acetone, methanol, glutaraldehyde solution(30%), toluene, and chlorobenzene of analytical grade were obtained from S.D. Fine Chemicals, India and used without any further purification.

2.2. Preparation of cross-linked PVA-AEAPTMEOS beads

PVA-AEAPTMEOS beads were prepared by acid-catalyzed sol–gel process and chemically cross-linked using glutaraldehyde as cross-linking agent. For acid-catalyzed sol–gel, desired amount of AEAPTMEOS (50.0, w/w silica content) was added to PVA solution (12.5%, w/w) in distilled water, and pH: 2.0 were maintained using 1.0 M HCl. The mixture was kept under stirred conditions at room temperature for 24 h to get clear sol solution. The resulting PVA-AEAPTMEOS solution (100 ml) was suspended in equal volume of toluene–chlorobenzene (1:3, v/v) containing Span-80 (3.0 ml) in a three-neck round bottom flask under continuous stirring (150 rpm) for 8 h at 30 °C. Then temperature was raised up to 90 °C for 8 h to distill out some part of water as an azeotrope with aromatic hydrocarbon. The resulting mixture was cooled at room temperature, and desired amount of glutaraldehyde solution (25%) in water (2%, w/w) was added as cross-linking agent. Then, it was stirred continuously for 8 h at room temperature to cross-link the water soluble suspended beads. The resulting beads were filtered, and washed several times with acetone followed *via* distilled water, and neutralized with 0.1 M NaOH followed by further washing.

2.3. FTIR and microscopic analysis

FTIR spectra of unloaded and loaded beads were recorded with spectrum GX series 49387 by KBr pellets method. For scanning electron microscopy (SEM), gold sputter coatings were carried out on the desired beads samples at pressure ranging in between 0.1 and 1.0 Pa. Images were recorded at 10^{-3} to 10^{-2} Pa EHT 15.00 kV with 300 V collector bias using Leo microscope. Transmission electron microscope (TEM) analysis was performed by JEOL 1200EDX with a tungsten filament electron source operated at an accelerating voltage of up to 120 kV. Pb(II) content in the adsorbed beads was detected by EDX measurements using LEO VP1430 and OXFORD INCA instrument.

2.4. Water content of PVA-AEAPTMEOS beads

Swelling of PVA-AEAPTMEOS beads was measured as water content (%). The dried beads of known weight in gram (W_{dry}) were suspended in deionized water under agitation for 24 h and weight of wet beads in gram (W_{wet}) was recorded. The percent water content in the beads was calculated using the following equation:

$$\text{Water content}(\%) = \frac{(W_{wet} - W_{dry})}{W_{dry}} \times 100 \quad (1)$$

2.5. Adsorption studies

The stock solution of Pb(II) (1000 ppm) was prepared by dissolving a known amount of $Pb(NO_3)_2$ in distilled water and batch process for the adsorption was carried out. A 0.5 g of dry beads was placed in a 50 ml solution with different Pb(II) concentrations in a conical flask. This was then placed in a shaker incubator at 100 rpm for desired time interval. The concentration of Pb(II) in the supernatant solution was determined by EDTA titration to estimate the adsorbed amount of Pb(II) [31]. Measuring error for the estimation of metal ion concentration was 0.1 mg/l. The amount of Pb(II) (q: mg g^{-1}) adsorbed on PVA-AEAPTMEOS beads was determined by following equation [32]:

$$q = \frac{(C_i - C_f)}{1000 \times W_{dry}} \times V \quad (2)$$

where C_i and C_f are the initial and final concentration of Pb(II) (mg/ml) before and after the adsorption, and V is the volume of Pb(II) solution (ml).

Adsorption studies were carried out at varied adsorbate concentration (10–200 mg/l), adsorption time (0.50–12.0 h), adsorbent dose (0.10–1.0 g) and temperature (30, 40 and 50 °C). Series of experiments were carried out using fixed amount of adsorbate at different pH (2.0–10.0).

2.6. Desorption studies

For desorption study, desired amount of adsorbent after Pb(II) adsorption was treated with, 0.10 M HCl, 0.10 M HNO_3, 0.10 M NaCl, oxalic acid and 0.01 M EDTA solution (50 ml of each), in a conical flask for 8 h. The desorbed amount of Pb(II) was determined by EDTA titration [31].

3. Results and discussions

3.1. Preparation and characterization of PVA-AEAPTMEOS beads

The PVA-AEAPTMEOS beads were prepared by condensation polymerization and acid-catalyzed sol–gel process. Gluteraldehyde was used as cross-linking agent. The cross-linking with gluteraldehyde is a two step process; hemiacetal was formed due to reaction between gluteraldehyde and hydroxyl groups of PVA. Further, it was reacted with another hydroxyl group and resulted acetal formation in second step. Reaction scheme for the preparation of PVA-AEAPTMEOS beads is presented in Scheme 1. The –NH_2/–NH groups of AEAPTMEOS were converted into salt by HCl treatment for their protection.

Structure of cross-linked PVA-AEAPTMEOS beads was assessed by FTIR spectra (Fig. 1), recorded before and after Pb(II) adsorption (A and B, respectively). The absorption bands at 2926 and 2857 cm^{-1} in spectrum A, and at 2925 and 2855 cm^{-1} in spectrum B are characteristic peaks due to –CH_2 symmetric and asymmetric stretching vibrations. The adsorption bands at 1642 (spectrum A), and 1647 cm^{-1} (spectrum B) are the characteristic peaks due to the –NH stretching vibrations. Under acidic condition, formation

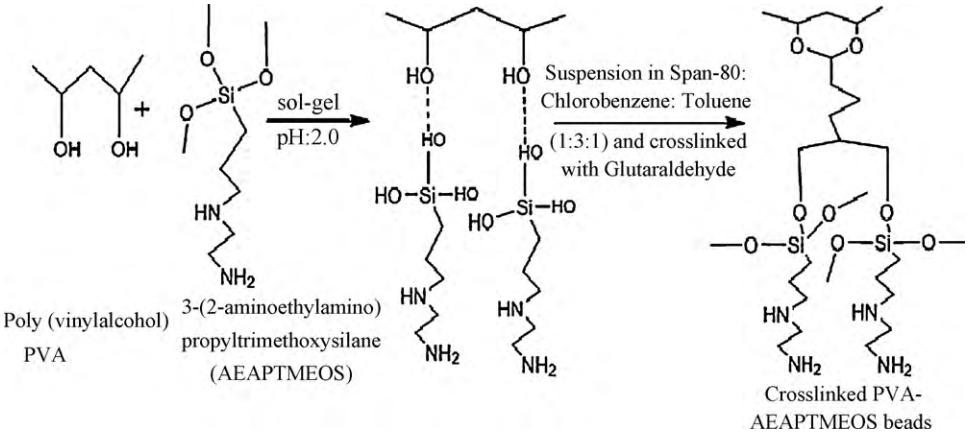

Scheme 1. Schematic reaction for the preparation of cross-linked PVA-AEAPTMEOS beads.

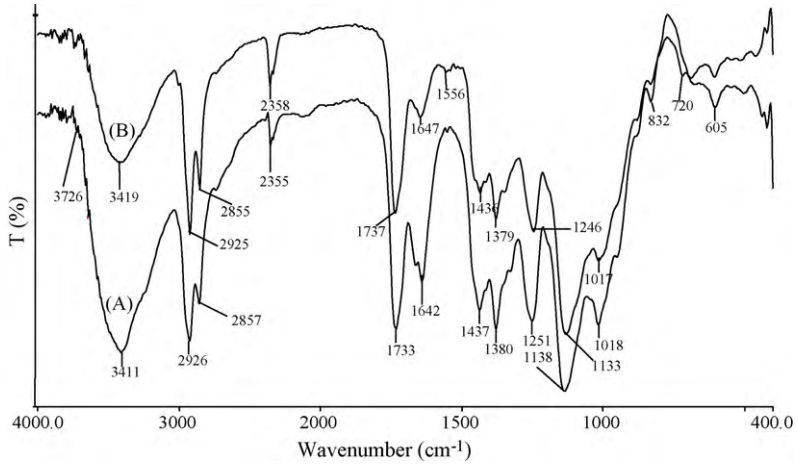

Fig. 1. FTIR spectra of PVA-AEAPTMEOS beads: (A) before and (B) after adsorption of Pb(II).

of C–O–C (~1251, 1246 cm^{-1} in spectrum A and B, respectively) and Si–O–C (1000–1200 cm^{-1}) favored the better compatibility between organic–inorganic components. The peaks in the range of 1015–1020 cm^{-1} for both spectrums, were assigned to Si–O–Si symmetric stretching vibrations [33]. The strong broad band at 3411 and 3419 cm^{-1} (for spectrum A and B, respectively) aroused due to the –NH stretching vibration in aliphatic amines. The significant reduction in transmittance of band at 3411 cm^{-1} after Pb(II) adsorption (spectra B) confirmed co-ordinate bonding between Pb(II) with $–NH_2$ and –NH [34]. The N–H bending vibrations at 1642 cm^{-1} (spectrum A) was shifted to 1647 cm^{-1} (spectrum B) after Pb(II) adsorption. Co-ordinate bonding between Pb(II) and active sites ($–NH_2$/–NH) was also supported by their Lewis acidic and basic nature, respectively. Thus $–NH_2$/–NH groups of silica precursor were acted as main active sites for the adsorption of Pb(II) from aqueous solution (Fig. 2).

Fig. 3(A and B) shows surface SEM images for PVA-AEAPTMEOS beads before and after Pb(II) adsorption. Spherical and rough surfaces of beads were responsible for high surface area and thus high Pb(II) adsorption (Fig. 3A). The morphology of beads surface was changed after Pb(II) adsorption, while it was retained after desorption of Pb(II). Fig. 4(A and B) presents TEM images of beads before and after Pb(II) adsorption, respectively. Nanosized homogeneously distributed silica can be observed (Fig. 4A), while its surface morphology was altered after Pb(II) adsorption (Fig. 4B). It was observed that active sites were occupied by Pb(II) adsorption via co-ordination as depicted in Fig. 4(C and D) which was confirmed by EDX study.

Swelling properties of PVA-AEAPTMEOS beads were assessed by water content. Prepared PVA-AEAPTMEOS beads were soluble in water without cross-linking, due to considerable hydrogen bonding with hydrophilic groups. After cross-linking, beads were water insoluble with lower degree of swelling (less than 1% dimensional change), which is important for their practical application in a column. However, after cross-linking PVA-AEAPTMEOS beads showed about 38.2% water content, which indicated its hydrophilic nature.

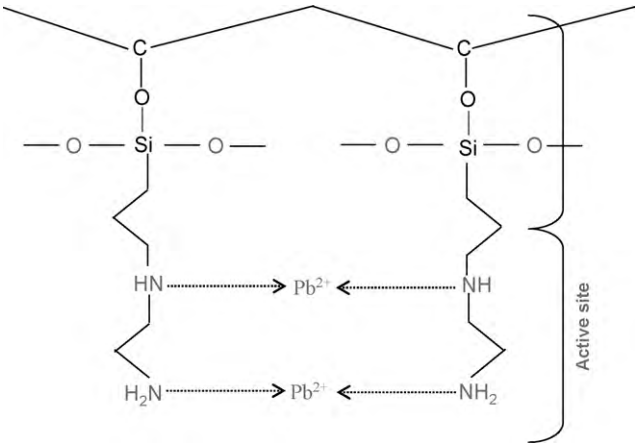

Fig. 2. Schematic presentation for Pb(II) adsorption on the active sites in PVA-AEAPTMEOS beads.

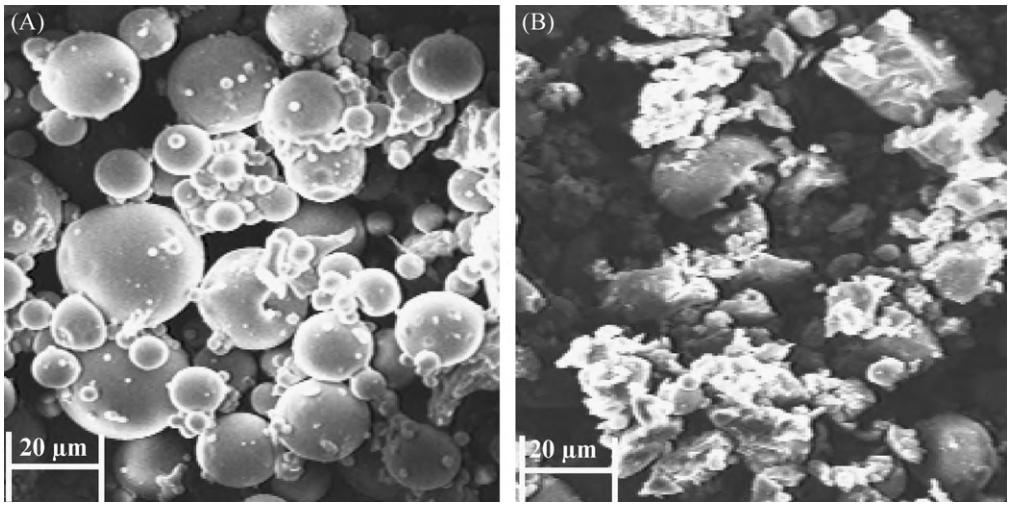

Fig. 3. SEM images of PVA-AEAPTMEOS beads: (A) unloaded and (B) loaded with Pb(II).

3.2. Effect of pH and contact time on Pb(II) adsorption

Several experiments were performed to optimize pH of the solution and contact time for maximum Pb(II) adsorption. Fig. 5A presents the effect of pH (2.0–10.0) on Pb(II) adsorption. About 23.3% adsorption of Pb(II) (50 mg/l) at pH: 2 was observed, which further increased to 76.2% at pH: 5.0, and attained a maximum value. In highly acidic medium, active sites of the adsorbent were protonated and reduced the metal ion adsorption capacity [1]. However, with increase in pH (deprotonation of $-NH_2$ and –NH

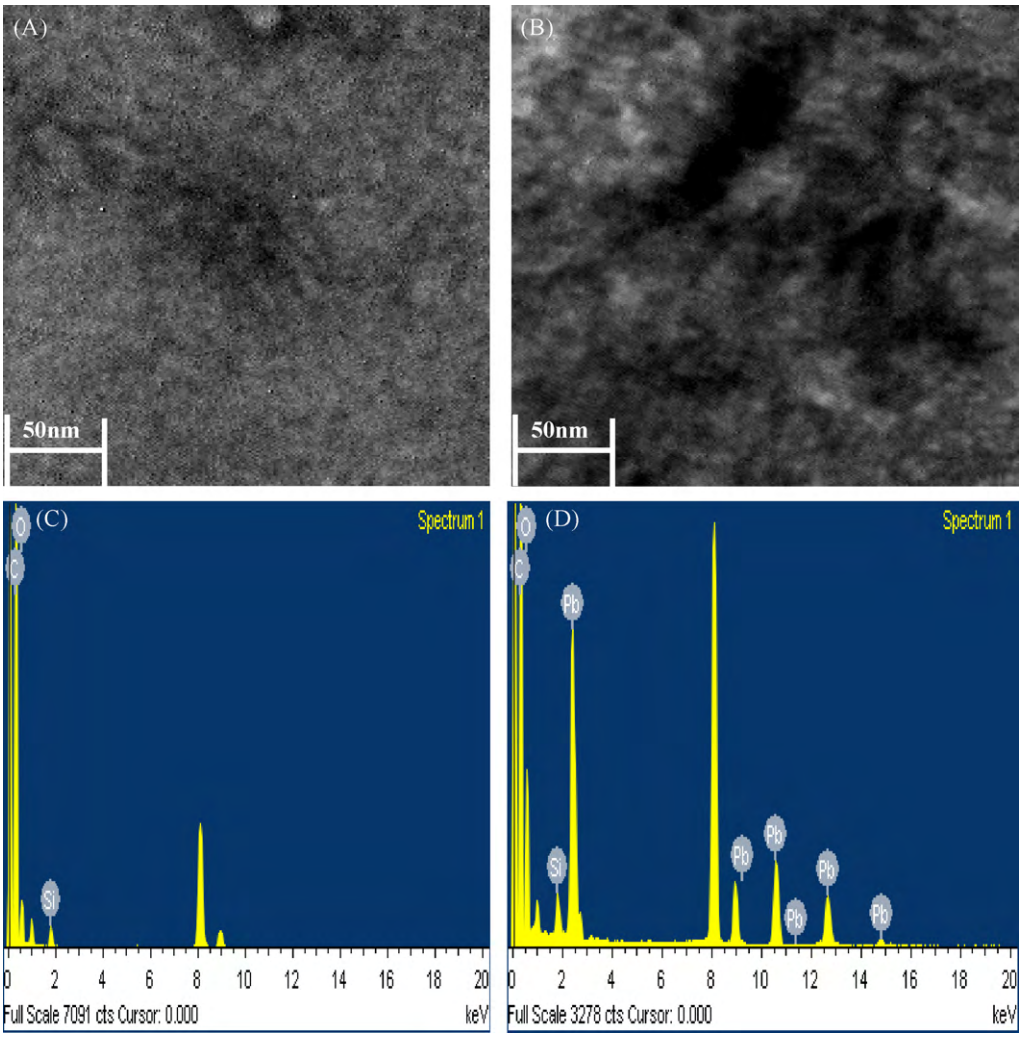

Fig. 4. TEM images of cross-linked PVA-AEAPTMEOS beads: (A) before and (B) after adsorption of Pb(II). (C) EDX spectrum of beads: (A) before and (D) after adsorption.

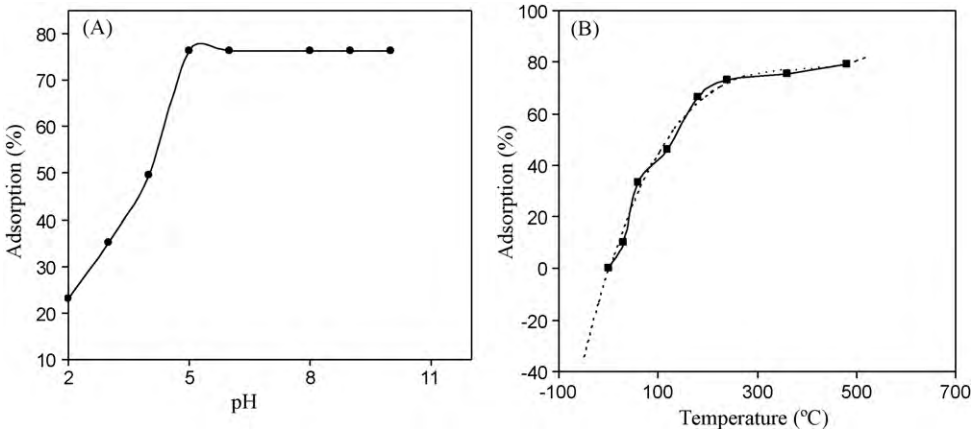

Fig. 5. (A) Effect of pH for Pb(II) (50 mg/l) adsorption and (B) effect of time on the adsorption capacity (%) for Pb(II) (50 mg/l; pH: 5.0).

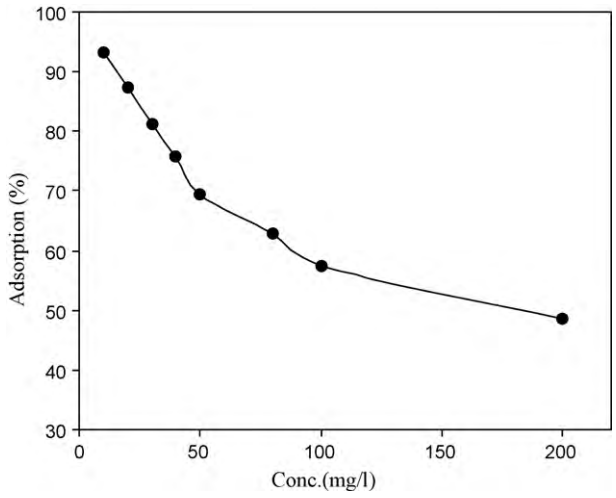

Fig. 6. Effect of initial Pb(II) concentration on adsorption by cross-linked PVA-AEAPTMEOS beads at pH: 5.0.

groups), adsorption increased and attained maximum at pH: 5.0. The solubility of metals decreases with increase in pH (in basic medium) and its precipitation starts. Thus, all adsorption studies were carried out in low acidic medium (pH: 5.0) to avoid the formation of Pb(II) hydroxide. Fig. 5B reveals that 4.0 h equilibrium time was required for the maximum removal of Pb(II) from water. Thus, subsequent adsorption studies were carried out at pH: 5.0 and 4.0 h equilibrium time. Initially, fast adsorption of Pb(II) occurred, may be due to the more number of available active sites, that reduced with time and attained a limiting value at equilibrium [35]. Adsorption capacity and time of equilibrium for an adsorbent are important parameters to assess its suitability for practical application [36]. Thus, about 76.2% of adsorption was achieved at 4.0 h equilibrium time, indicating the efficiently use of the developed beads for the removal of Pb(II) from wastewater.

3.3. Effect of Pb(II) concentration and adsorbent dose

Cross-linked PVA-AEAPTMEOS beads are an effective adsorbent over a wide concentration range of adsorbate (Pb(II)) at pH: 5.0. At lower Pb(II) concentration (10 mg/l), beads showed ~93% adsorption, which reduced with increase in Pb(II) initial concentration (Fig. 6). 77.3% adsorption was observed at 50 mg/l Pb(II) concentration,. Thus, developed beads are more suitable for the removal of Pb(II) (10–50 mg/l) with lower concentration from aqueous solution. Furthermore, one has to optimize the adsorbent dose depending on the concentration of adsorbate and pH for maximum utilization of the adsorbent.

At pH: 5.0, adsorption (%) of cross-linked PVA-AEAPTMEOS beads for the removal of Pb(II) (50 mg/l) from aqueous solution are presented as a function of adsorbent dose (0.1–1.0 g) at constant temperature (Fig. 7). Adsorption capacity decreased (39.3–11.60 mg g^{-1}) with the increase in adsorbent dose. The observed reduction in adsorption capacity of the developed beads may be attributed due to availability of less active site at high adsorbent dose.

3.4. Adsorption mechanism

In cross-linked PVA-AEAPTMEOS beads, N atoms of active sites (–NH/–NH_2) were responsible for the complexation of Pb(II), due to the availability of lone pair of electrons. Following chemical reactions are proposed for Pb(II) adsorption and desorption mechanism [1,8]:

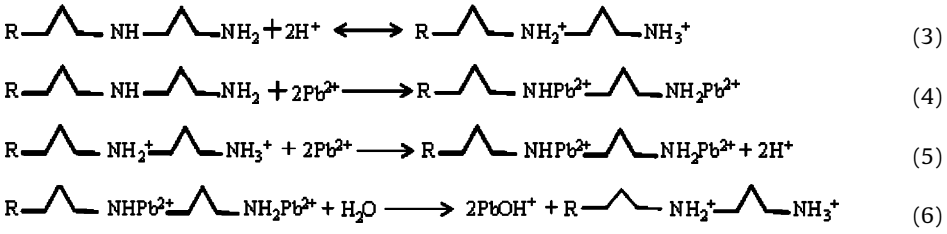

The equilibrium reaction (Eq. (3)) was established *via* pH of initial adsorbate solution. Pb^{2+} adsorption occurred on active sites (–NH/–NH_2) of the developed beads through co-ordinate bond. In this case active sites acted as Lewis base, while Pb^{2+} acted as Lewis acid (Eq. (4)) in comparison with H^+ and nitrogen atoms (i.e., protonation of the available –NH_2 and –NH active sites in the beads). Eq. (5) governs the difference in the binding capacity of nitrogen atoms with Pb^{2+} or H^+, and a competitive adsorption of Pb^{2+} takes place over H^+ ions. Thus, adsorption process can also be termed as an ion-exchange mechanism [37]. However,

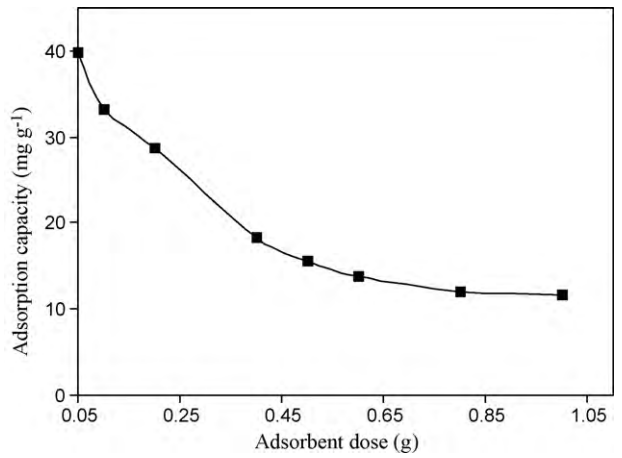

Fig. 7. Effect of adsorbent dose for Pb(II) (50 mg/l) adsorption on cross-linked PVA-AEAPTMEOS beads at pH: 5.0.

resulting reaction (Eq. (5)) may be slower than those presented in Eq. (4), because of less attraction R–NH_2^+–NH_3^+ between R–NH–NH_3 and Pb^{2+} in comparison with R–$NHPb^{2+}$–NH_2Pb^{2+} and Pb^{2+}. Formation of $PbOH^+$ from complex (Eq. (6)) occurred due to the greater the electrostatic interaction between Pb^{2+} with OH^- ion in comparison with nitrogen atoms available in active sites of the developed beads. Thus adsorption occurred mainly due to the complexation between Pb^{2+} and $–NH_2$ and –NH active sites present in the developed beads.

3.5. Adsorption kinetics

The rate constants were calculated from pseudo-first- and second-order kinetic models [1]. The first-order expression is given as:

$$\log(q_e - q) = \log q_e - \frac{K_1}{2.303} t \tag{7}$$

q_e is the amount adsorbed (mg g^{-1}) at equilibrium, and q is the amount adsorbed after time t (min). K_1 (min^{-1}) first-order rate constant that was estimated from the slope of $\log(q_e - q)$ versus t linear plots at different concentrations (Fig. 8(A)), and presented along with correlation coefficient (R^2) in Table 1. The rate equation for pseudo-second-order kinetic model is given as:

$$\frac{t}{q} = \frac{1}{h} + \left(\frac{1}{q_e}\right) t \tag{8}$$

where $h = K_2 q_e^2$ and K_2 is the rate constant for pseudo-second-order adsorption (g mg^{-1} min^{-1}). The values of h were estimated from the intercept of t/q versus t plots presented in (Fig. 8 (B)), and included in Table 1 along with K_2 (g mg^{-1} min^{-1}), and R^2 values. The R^2 values for pseudo-second-order kinetic were slightly higher than the pseudo-first-order kinetic. This indicated better obeyed pseudo-second-order kinetic as compared to pseudo-first-order kinetic under studied concentration range (20–100 mg/l) [1].

3.6. Effect of temperature

The Pb(II) adsorption was also assessed at different temperatures (30–50 °C) and thermodynamic parameters such as free energy change (ΔG°), enthalpy change (ΔH°) and entropy change (ΔS°) were estimated by following equations [1]:

$$K_c = \frac{C_{Ac}}{C_e} \tag{9}$$

where K_c is the equilibrium constant, C_{Ac} and C_e are equilibrium concentrations (mg/l) of Pb(II) on the beads and in solution, respectively:

$$\Delta G^0 = -2.303RT \log K_C \tag{10}$$

$$\log K_C = \left(\frac{\Delta S^\circ}{2.303R}\right) - \left(\frac{\Delta H^\circ}{2.303RT}\right) \tag{11}$$

where T is the absolute temperature (K) and R is the universal gas constant. Values of ΔS° and ΔH° were estimated at 40 °C from the slope and intercept of van't Hoff plot ($\log K_c$ versus $1/T$) between 30 and 50 °C (Fig. 9) and the data was included in Table 2. While these values at 30 and 50 °C were determined from slope and intercept of van't Hoff plot between 30–40 and 40–50 °C, respectively. Results revealed that Pb(II) adsorption was endothermic, and spontaneous. Positive values of ΔS° suggested an increase in randomness at the solid–solution interface during adsorption [2,38,39].

3.7. Adsorption isotherms

The adsorption isotherm model describes the interaction between adsorbate with adsorbent, knowledge of which is essential for maximum utilization of the adsorbent. To correlate the equilibrium data by empirical models is essential for designing a perfect adsorption operating process. In the present study, the data at equilibrium were derived from the linear fit of Freundlich (Eq. (12)) and Langmuir (Eq. (13)) isotherms for the adsorption of Pb(II) [1,40,41]:

$$\log q_e = \log K_F + \frac{1}{n} \log C_e \tag{12}$$

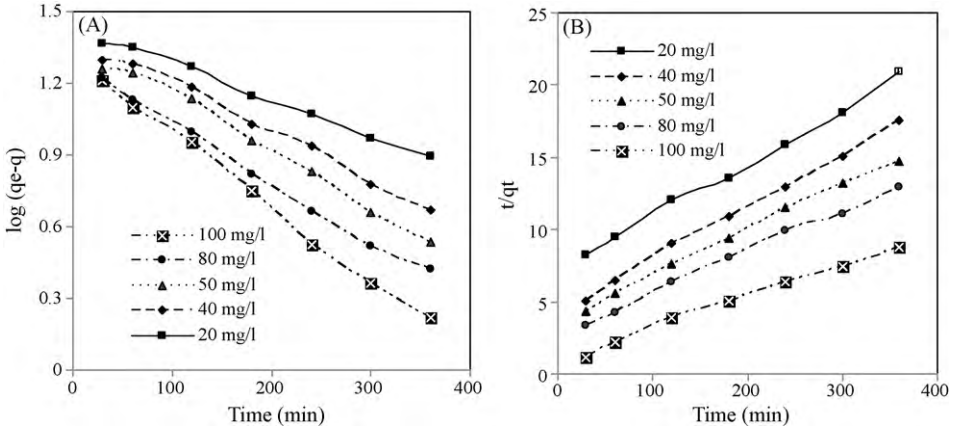

Fig. 8. (A) Pseudo-first-order and (B) second-order kinetics plots for Pb(II) adsorption at different concentrations at pH: 5.0 (adsorbent dose: 0.50 g).

Table 1
Pseudo-first- and second-order kinetics constants, correlation coefficients (R^2) for the adsorption of Pb(II) on cross-linked PVA-AEAPTMEOS beads.

Conc. (mg/l)	Pseudo-first-order kinetics		Pseudo-second-order kinetics			
	K_1 (min^{-1})	R^2	K_2 (g mg^{-1} min^{-1})	q_e (mg g^{-1})	h (mg g^{-1})	R^2
20	0.0031	0.9902	0.000192	26.88	0.139	0.9961
40	0.0025	0.9957	0.000253	28.38	0.255	0.9948
50	0.0023	0.9840	0.000291	32.49	0.266	0.9835
80	0.0019	0.9863	0.000368	35.09	0.358	0.9921
100	0.0015	0.9925	0.000605	44.45	1.120	0.9922

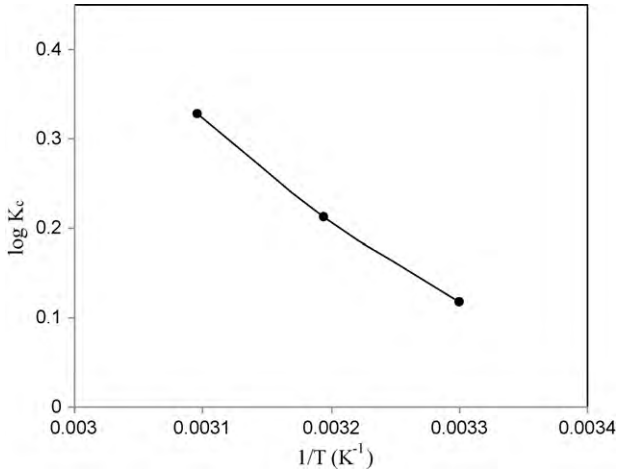

Fig. 9. Plot of log K_c versus $1/T$ for the adsorption of Pb(II) (50 mg/l) on cross-linked PVA-AEAPTMEOS beads at pH: 5.0.

Table 2
Thermodynamic parameters and correlation coefficients (R^2) at different temperatures for Pb(II) adsorption.

Temp (°C)	ΔS° (kJ K^{-1} mol^{-1})	ΔH° (kJ mol^{-1})	ΔG° (kJ mol^{-1})	R^2
30	0.059	17.23	−0.67	–
40	0.067	19.72	−1.33	0.9942
50	0.076	22.45	−2.03	–

Table 3
Freundlich and Langmuir constants and correlation coefficients (R^2) for Pb(II) adsorption.

Temp (°C)	Freundlich constants			Langmuir constants			
	K_F	$1/n$	R^2	a_L	K_L	Q_0 (mg g^{-1})	R^2
30	7.16	0.567	0.972	0.073	4.94	67.56	0.985
40	9.14	0.564	0.985	0.097	7.11	72.99	0.992
50	13.61	0.526	0.990	0.167	12.76	76.33	0.998

$$\frac{C_e}{q_e} = \frac{1}{K_L} + \frac{a_L}{K_L} C_e \quad (13)$$

where C_e is Pb(II) concentration (mg/l) in solution at equilibrium, K_F is Freundlich constant and $1/n$ is the heterogeneity factor, while a_L and K_L are Langmuir constants.

Freundlich isotherm describes the heterogeneous system and reversible adsorption. This is not restricted to the monolayer formation on the adsorbent surfaces. This is also described an increase Pb(II) adsorption with initial adsorbate concentration in solution [1,42,43]. For Langmuir isotherms, it was assumed that intermolecular forces were rapidly reduced with distance and thus led to the monolayer formation on the adsorbent surface [5]. Furthermore, no adsorption took place after adsorption on the active sites of the adsorbent [36]. Freundlich constants and R^2 values were obtained from Freundlich isotherms (Fig. 10A) and data are presented in Table 3. Deviation from linearity (under study concentration range is taken into the consideration) may be attributed to either: (i) availability of other active sites for the adsorption that produced irregular energy distribution in the adsorbent, or (ii) purely physical adsorption [1,36,41].

Langmuir constants (K_L) and R^2 values were derived from Langmuir isotherms and data, are also presented in Table 3. Langmuir isotherms were well correlated ($R^2 = 0.998$) in compare with Freundlich isotherms ($R^2 = 0.990$) (Fig. 10B). Increase in a_L values with temperature, indicated the strong binding of Pb(II) with –NH_2/–NH active sites in the developed beads [36]. It was observed that the adsorption capacity (monolayer saturation capacity; Q_0) increased with the temperature [41]. Q_0 value for an adsorption process is a measure of monolayer adsorption capacity of adsorbents. Our experimental findings were compared with the reported Q_0 values (26.5–58.9 mg g^{-1}) in literature [44–50]. While, 67.6 mg g^{-1} Q_0 value (observed in this study), revealed the superiority of developed cross-linked PVA-AEAPTMEOS beads for Pb(II) adsorption.

The essential feature of Langmuir isotherms can be expressed as dimensionless constant (separation factor) or equilibrium param-

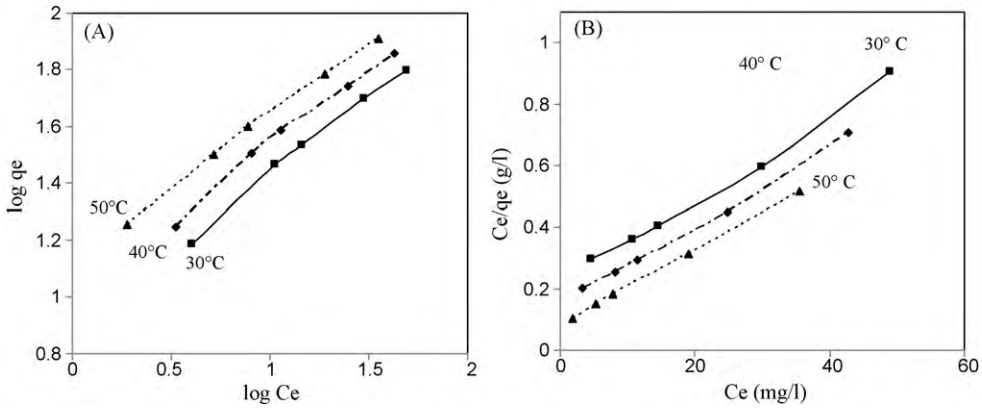

Fig. 10. (A) Freundlich and (B) Langmuir isotherms, for Pb(II) adsorption on cross-linked PVA-AEAPTMEOS beads.

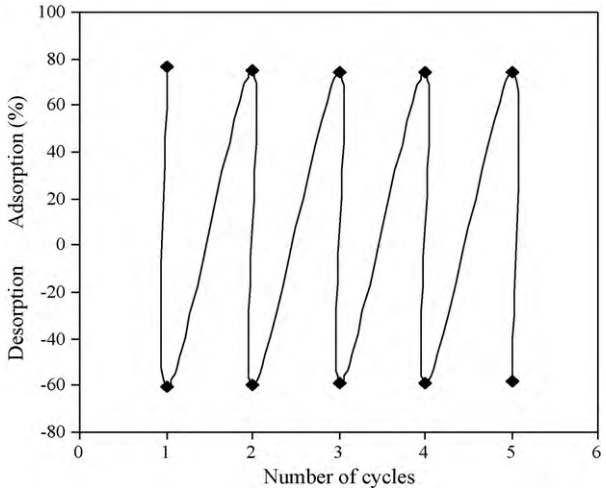

Fig. 11. Adsorption and desorption studies for the Pb (II) on the developed PVA-AEAPTMEOS beads (concentration; 50 mg/l, pH: 5.0).

eter (R_L) estimated by:

$$R_L = \frac{1}{1 + K_L C_0} \quad (14)$$

where K_L is the Langmuir constant and C_0 is the initial Pb(II) concentration (mg/l). The R_L values were estimated and found to be varied between 0.910 and 0.105 under different experimental conditions, which indicated favorable Pb(II) adsorption on the beads [1].

3.8. Desorption studies

Desorption studies revealed feasibility of desorption process to recover of Pb(II) from the adsorbent after adsorption of adsorbate. Oxalic acid, H_2SO_4, HCl, HNO_3, NaCl and EDTA solution were used for desorption of Pb(II) from PVA-AEAPTMEOS beads. Desorption of Pb(II) followed the trend: HCl(20.1%) < HNO_3(42.3) < EDTA(60.2%). Furthermore, for developed materials, number of adsorption and desorption cycles were analyzed using 50 mg/l Pb(II) solution at pH: 5.0 with 0.5 g adsorbent dose, while desorption studies were carried out by EDTA solution. Results presented in Fig. 11, revealed that developed material can be efficiently used up to five numbers of cycles with negligible loss (1–2%) in adsorption and desorption capacity.

4. Conclusions

Cross-linked PVA-AEAPTMEOS beads with low degree of swelling were prepared by condensation polymerization followed acid-catalyzed sol–gel in presence of non-ionic surfactant. It was observed that cross-linking, reduced the swelling (38.2%, w/w) and enhanced the chemical stability of the developed beads in acidic medium. Developed beads were utilized for Pb(II) removal from aqueous solution. The kinetic data showed well fitted pseudo-second-order kinetic in compared to pseudo-first-order kinetic, due to the better correlation with the experimental data. The Langmuir and Freundlich isotherms, both indicated favorable Pb(II) adsorption. Developed beads exhibited 76.2% Pb(II) adsorption for 4.0 h equilibrium time (initial concentration: 50 mg/l; pH: 5.0).

Superiority of cross-linked PVA-AEAPTMEOS beads over reported adsorbents was revealed from Pb(II) adsorption capacity values. About 60.2% recovery of Pb(II) (in EDTA) was achieved by desorption study in 0.01 M solution (HCl, HNO_3 and EDTA), while desorption was not possible in NaCl and oxalic acid. Adsorption occurred mainly via complexation of Pb(II) with available active sites in beads. Furthermore, desorption studies suggested that the developed cross-linked PVA-AEAPTMEOS beads can be effectively utilized for the removal of Pb(II) from wastewater.

Acknowledgements

Authors are extremely thankful to the BNRS, DAE, Govt. of India, for providing financial assistance by sanctioning project no. 2007/35/35/BNRS/102. We also acknowledge the services of Analytical Science Division, CSMCRI, Bhavnagar for instrumental support.

References

[1] M. Kumar, B.P. Tripathi, V.K. Shahi, Crosslinked chitosan/polyvinyl alcohol blend beads for removal and recovery of Cd(II) from wastewater, J. Hazard. Mater. 172 (2009) 1041–1048.
[2] U. Ulusoy, S. Simsek, Lead removal by polyacrylamide–bentonite and zeolite composites: effect of phytic acid immobilization, J. Hazard. Mater. B127 (2005) 163–171.
[3] P.C. Mishra, R.K. Patel, Removal of lead and zinc ions from water by low cost adsorbents, J. Hazard. Mater. 168 (2009) 319–325.
[4] X. Bi, R.J. Lau, K.-L. Yang, Preparation of ion-impregnated silica gels, functionalized with glycine, dyglycine, and triglycine and their adsorption properties for copper ions, Langmuir 23 (2007) 8079–8096.
[5] C.A Quirarte-Escalante, V. Soto, W. del Cruz, G.R. Porras, R. Manriquez, S. Gomez-Salazar, Synthesis of hybrid adsorbents combining sol–gel processing and molecular imprinting applied to lead removal from aqueous streams, Chem. Mater. 21 (2009) 1439–1450.
[6] USEPA Nutrient Criteria Technical Guidance Manual: Lakes and Reservoirs, United States Environmental Protection Agency (USEPA), Washington, DC, 1999 (Document EPA 822).
[7] World Health Organization, Guidelines for Drinking Water Quality, vol. 1 Recommendations, 2nd ed., World Health Organization (WHO), Geneva, Switzerland, 1993.
[8] L. Jin, R. Bai, Mechanisms of lead adsorption on chitosan/PVA hydrogel beads, Langmuir 18 (2002) 9765–9770.
[9] F. Banat, S.A. Asheh, L. Makhadmeh, Kinetics and equilibrium study of cadmium ion sorption onto date pits—an agricultural waste, Adsorpt. Sci. Technol. 21 (2003) 245–260.
[10] N.V. Narayanan, M. Ganesan, Use of adsorption using granular activated carbon (GAC) for the enhancement of removal of chromium from synthetic wastewater by electrocoagulation, J. Hazard. Mater. 161 (2009) 575–580.
[11] S. Boussetta, C. Branger, A. Margaillan, J.-L. Boudenne, B. Coulomb, Salicylic acid and derivatives anchored on poly(styrene-co-divinylbenzene) resin and membrane via a diazo bridge: synthesis, characterization and application to metal extraction, React. Funct. Polym. 68 (2008) 775–786.
[12] H. Hyung, J.-H. Kim, Mechanistic study on boron rejection by sea water reverse osmosis membranes, J. Membr. Sci. 286 (2006) 269–278.
[13] X.J. Zhang, T.Y. Ma, Z.Y. Yuan, Titania–phosphonate hybrid porous materials: preparation, photocatalytic activity and heavy metal ion adsorption, J. Mater. Chem. 18 (2008) 2003–2010.
[14] C. Barthet, A.J. Hickey, D.B. Cairns, S.P. Armes, Synthesis of novel polymer–silica colloidal nanocomposites via free-radical polymerization of vinyl monomers, Adv. Mater. 11 (1999) 408–410.
[15] J. Liu, X. Wang, T. Xu, G. Shao, Novel negatively charged hybrids. 1. Copolymers: preparation and adsorption properties, Sep. Purif. Technol. 66 (2009) 135–142.
[16] C. Xiong, C. Yao, Synthesis, characterization and application of triethylenetetramine modified polystyrene resin in removal of mercury, cadmium and lead from aqueous solutions, Chem. Eng. J. 155 (2009) 844–850.
[17] V.K. Gupta, C.K. Jain, V. Ali, S. Chandra, S. Agarwal, Removal of lindane and malathion from wastewater using bagasse fly ash—a sugar industry waste, Water Res. 36 (2002) 2483–2490.
[18] H.J. Fornwalt, R.A. Hutchins, Purifying liquids with activated carbon, Chem. Eng. 73 (1966) 179–183.
[19] M. Li, S. Cheng, H. Yan, Preparation of crosslinked chitosan/poly(vinyl alcohol) blend beads with high mechanical strength, Green Chem. 9 (2007) 894–898.
[20] L. Zhao, H. Mitomo, M. Zhai., F. Yoshii, N. Nagasawa, T. Kume, Synthesis of antibacterial PVA/CM-chitosan blend hydrogels with electron beam irradiation, Carbohydr. Polym. 53 (2003) 439–446.
[21] H. Zou, S. Wu, J. Shen, Polymer/silica nanocomposites: preparation, characterization, properties, and applications, Chem. Rev. 108 (2008) 3893–3957.
[22] L. Depre, M. Ingram, C. Poinsignon, M. Popall, Proton conducting sulfon/sulfon amide functionalized materials based on inorganic–organic matrices, Electrochim. Acta 45 (2000) 1377–1383.
[23] V.V. Binsu, R.K. Nagarale, V.K. Shahi, Phosphonic acid functionalized aminopropyl triethoxysilane–PVA composite material: organic–inorganic hybrid proton-exchange membranes in aqueous media, J. Mater. Chem. 15 (2005) 4823–4831.
[24] P. Stathi, K. Dimos, M.A. Karakassides, Y. Deligiannakis, Mechanism of heavy metal uptake by a hybrid MCM-41 material: surface complexation and EPR spectroscopic study, J. Colloid Interf. Sci. 343 (2010) 374–380.

[25] Q. Su, B. Pan, B. Pan, Q. Zhang, W. Zhang, L. Lv, X. Wang, J. Wu, Q. Zhang, Fabrication of polymer-supported nanosized hydrous manganese dioxide (HMO) for enhanced lead removal from waters, Sci. Total Environ. 407 (2009) 5471–5477.
[26] M. Arkas, D. Tsiourvas, Organic/inorganic hybrid nanospheres based on hyperbranched poly(ethyleneimine) encapsulated into silica for the sorption of toxic metal ions and polycyclic aromatic hydrocarbons from water, J. Hazard. Mater. 170 (2009) 35–42.
[27] J. Liu, Y. Ma, Y. Zhang, G. Shao, Novel negatively charged hybrids. 3. Removal of Pb^{2+} from aqueous solution using zwitterionic hybrid polymers as adsorbent, J. Hazard. Mater. 173 (2010) 438–444.
[28] M.E. Mahmoud, O.F. Hafez, M.M. Osman, A.A. Yakout, A. Alrefaay, Hybrid inorganic/organic alumina adsorbents-functionalized-purpurogallin for removal and preconcentration of Cr(III), Fe(III), Cu(II), Cd(II) and Pb(II) from underground water, J. Hazard. Mater. 176 (2010) 906–912.
[29] K. Dimos, P. Stathi, M.A. Karakassides, Y. Deligiannakis, Synthesis and characterization of hybrid MCM-41 materials for heavy metal adsorption, Micropor. Mesopor. Mater. 126 (2009) 65–71.
[30] R. Ballesteros, D. Perez-Quintanilla, M. Fajardo, I. del Hierro, I. Sierra, Adsorption of heavy metals by pirymidine-derivated mesoporous hybrid material, J. Porous Mater. (2009), doi:10.1007.
[31] J. Bassett, R.C. Denney, G.H. Jeffery, J. Mendham, Vogel's Textbook Quantitative Inorganic Analysis, 4th ed., 1978, pp. 316–319.
[32] S. Jacob, S. Cohet, C. Poinsignon, M. Popall, Proton conducting inorganic–organic matrices based on sulfonyl- and styrene derivatives functionalized polycondensates via sol–gel processing, Electrochim. Acta 48 (2003) 2181–2186.
[33] W.S.W. Ngah, C.S. Endud, R. Mayanar, Removal of copper(II) ions from aqueous solution onto chitosan and cross-linked chitosan beads, React. Funct. Polym. 50 (2002) 181–190.
[34] T.-Y. Hsien, G.L. Rorrer, Heterogeneous cross-linking of chitosan gel beads: kinetics, modeling, and influence on cadmium ion adsorption capacity, Ind. Eng. Chem. Res. 36 (1997) 3631–3638.
[35] B. Xiao, K.M. Thomas, Adsorption of aqueous metal ions on oxygen and nitrogen functionalized nanoporous activated carbons, Langmuir 21 (2005) 3892–3902.
[36] D.N. Bajpai, Advanced Physical Chemistry, S. Chand and Company, New Delhi, India, 1998.
[37] A. Saeed, M. Iqbal, M.W. Waheed, Removal and recovery of lead(II) from single and multimetal (Cd, Cu, Ni, Zn) solutions by crop milling waste (black gram husk), J. Hazard. Mater. B 117 (2005) 65–73.
[38] W. Plazinski, W. Rudzinski, Modeling the effect of pH on kinetics of heavy metal ion biosorption. A theoretical approach based on the statistical rate theory, Langmuir 25 (2009) 298–304.
[39] S.H. Jang, Y.G. Jeong, B.G. Min, W.S. Lyoo, S.C. Lee, Preparation and lead ion removal property of hydroxyapatite/polyacrylamide composite hydrogels, J. Hazard. Mater. 159 (2008) 294–299.
[40] S. Deng, R. Bai, J.P. Chen, Aminated polyacrylonitrile fibers for lead and copper removal, Langmuir 19 (2003) 5058–5064.
[41] A. Corami, S. Mignardi, V. Ferrini, Cadmium removal from single- and multimetal ($Cd^{2+} + Pb^{2+} + Zn^{2+} + Cu^{2+}$) solutions by sorption on hydroxyapatite, J. Colloid Interf. Sci. 317 (2008) 402–408.
[42] A. Duran, M. Soylak, S.A. Tuncel, Poly(vinyl pyridine–poly ethylene glycol methacrylate–ethylene glycoldimethacrylate) beads for heavy metal removal, J. Hazard. Mater. 155 (2008) 114–120.
[43] Y. Xu, D. Zhao, Removal of lead from contaminated soils using poly(amidoamine) dendrimers, Ind. Eng. Chem. Res. 45 (2006) 1758–1765.
[44] M. Sekar, V. Sakthi, S. Rengaraj, Kinetics and equilibrium adsorption study of lead(II) onto activated carbon prepared from coconut shell, J. Colloid Interf. Sci. 279 (2004) 307–313.
[45] A.R. Khalaf, H.M. Al-Najar, J.T. Hamed, Assessment of rainwater run-off due to the proposed regional plan for gaza governorates, J. Appl. Polym. Sci. 6 (2006) 2762–2767.
[46] M. Kobya, E. Demirbas, E. Senturk, M. Ince, Adsorption of heavy metal ions from aqueous solutions by activated carbon prepared from apricot stone, Bioresour. Technol. 96 (2005) 1518–1521.
[47] E. Eren, Removal of lead ions by Unye (Turkey) bentonite in iron and magnesium oxide-coated forms, J. Hazard. Mater. 165 (2009) 63–70.
[48] E. Eren, B. Afsin, Y. Onal, Removal of lead ions by acid activated and manganese oxide-coated bentonite, J. Hazard. Mater. 161 (2009) 677–685.
[49] R. Balasubramanian, S.V. Perumal, K. Vijayaraghavan, Equilibrium isotherm studies for the multicomponent adsorption of lead, zinc, and cadmium onto Indonesian peat, Ind. Eng. Chem. Res. 48 (2009) 2093–2099.
[50] J. Goel, K. Kadirvelu, C. Rajagopal, V.K. Garg, Removal of lead(II) from aqueous solution by adsorption on carbon aerogel using a response surface methodological approach, Ind. Eng. Chem. Res. 44 (2005) 1987–1994.